energies

MDPI

Article

Effects of Structural Substituents on the Electrochemical Decomposition of Carbonyl Derivatives and Formation of the Solid–Electrolyte Interphase in Lithium-Ion Batteries

S. Hamidreza Beheshti [1,2,*], Mehran Javanbakht [2], Hamid Omidvar [3], Hamidreza Behi [1], Xinhua Zhu [4], Mesfin Haile Mamme [4], Annick Hubin [4], Joeri Van Mierlo [1] and Maitane Berecibar [1]

1 Research Group MOBI–Mobility, Logistics and Automotive Technology Research Centre, Vrije Universiteit Brussel, 1050 Brussels, Belgium; Hamidreza.Behi@VUB.be (H.B.); joeri.van.mierlo@vub.be (J.V.M.); Maitane.Berecibar@vub.be (M.B.)
2 Department of Chemistry, Amirkabir University of Technology, Tehran 159163-4311, Iran; javanbakht@aut.ac.ir
3 Department of Mining and Metallurgical Engineering, Amirkabir University of Technology, Tehran 159163-4311, Iran; omidvar@aut.ac.ir
4 Electrochemical and Surface Engineering Group, Department of Materials and Chemistry, Vrije Universiteit Brussel, 1050 Brussels, Belgium; Xinhua.zhu@vub.be (X.Z.); Mesfin.Haile.Mamme@vub.be (M.H.M.); Annick.Hubin@vub.be (A.H.)
* Correspondence: Seyed.Hamidreza.Beheshti@vub.be

Abstract: The solid–electrolyte interphase (SEI), the passivation layer formed on anode particles during the initial cycles, affects the performance of lithium-ion batteries (LIBs) in terms of capacity, power output, and cycle life. SEI features are dependent on the electrolyte content, as this complex layer originates from electrolyte decomposition products. Despite a variety of studies devoted to understanding SEI formation, the complexity of this process has caused uncertainty in its chemistry. In order to clarify the role of the substituted functional groups of the SEI-forming compounds in their efficiency and the features of the resulting interphase, the performance of six different carbonyl-based molecules has been investigated by computational modeling and electrochemical experiments with a comparative approach. The performance of the electrolytes and stability of the generated SEI are evaluated in both half-cell and full-cell configurations. Added to the room-temperature studies, the cyclability of the NMC/graphite cells is assessed at elevated temperatures as an intensified aging condition. The results show that structural adjustments within the SEI-forming molecule can ameliorate the cyclability of the electrolyte, leading to a higher capacity retention of the LIB cell, where cinnamoyl chloride is introduced as a novel and more sustainable SEI forming agent with the potential of improving the LIB capacity retention.

Keywords: solid–electrolyte interphase; electrolyte additive; molecular tunning; SEI stability; irreversible capacity loss; lithium-ion battery

check for updates

Citation: Beheshti, S.H.; Javanbakht, M.; Omidvar, H.; Behi, H.; Zhu, X.; Mamme, M.H.; Hubin, A.; Van Mierlo, J.; Berecibar, M. Effects of Structural Substituents on the Electrochemical Decomposition of Carbonyl Derivatives and Formation of the Solid–Electrolyte Interphase in Lithium-Ion Batteries. *Energies* **2021**, *14*, 7352. https://doi.org/10.3390/en14217352

Academic Editor: Alvaro Caballero

Received: 1 October 2021
Accepted: 28 October 2021
Published: 4 November 2021

Publisher's Note: MDPI stays neutral with regard to jurisdictional claims in published maps and institutional affiliations.

1. Introduction

The lithium-ion battery (LIB) has been a disruptive technology that has introduced new trends and possibilities to the energy sector, namely the emerging market of electric vehicles. In order to fulfill the demands of such applications, LIBs require continuous improvement in terms of capacity, power output, life cycle, and safety. The formation of a decent solid–electrolyte interphase (SEI), an ion-passing and electron-blocking layer which covers the anode particles from the initial cycles, is an approach to ameliorate these features, leading to a more efficient LIB cell [1,2]. The SEI is composed of electrolyte decomposition products where the reduction process of the solvent molecules proceeds with the consumption of Li^+ ions, resulting in an irreversible capacity loss (ICL) [3,4].

Studies have shown that however the SEI is primarily formed within the early cycles (formation cycles), the decomposition mechanisms continue due to the physical defects or the electrochemical instability of the initial interphase, leading to a gradual SEI evolution [5]. Therefore, instability of the decomposition products would result in an extended continuation of the degradative mechanisms and a further decrease in lithium inventory [6]. The instability of lithium-alkyl carbonates, a frequently detected SEI component in carbonate electrolytes [7,8], and their transformation to the other interfacial species is reported as an example of the interphase evolution process [5]. Investigations have revealed the evolved SEI as a two-sectioned layer constructed from a mainly inorganic part adjacent to the electrode and a mainly organic section close to the electrolyte [9–11]. Formation of stable inorganic species like LiF and Li_2CO_3 [12,13], as well as the generation of polymeric structures in the organic section [14,15], has been reported as a pathway to stabilize the SEI, resulting in better capacity retention.

Introducing SEI-forming agents to the electrolyte is a promising method to modify the reduction products in order to protect the electrolyte from long-term decomposition and consequently improve LIB stability [6,16–21]. The employed additives reduce at the anodic side prior to the solvent molecules. A group of these reagents is polymerizable compounds with unsaturated bonds in their structures which can form the SEI through a polymerization reaction via nucleophilic addition [16]. Considering the variant electrochemical properties of different organic groups, a diverse range of structures based on carbonates [12,13,22–28], anhydrides [29], nitriles [30–33], isocyanates [15,34], sulfones, and sulfonates [35–38] are studied in SEI formation. Some recent works have followed SEI improvement by introducing a class of additives containing various functional groups. Among these, p-toluenesulfonyl isocyanate [17], 3-(phenylsulfonyl) propionitrile [18], fluorosulfonyl isocyanate [19], and, p-toluenesulfonyl methyl isocyanide [20] could be mentioned as examples which contain different nitrogen-based and sulfur-based groups in their molecular structures. Despite the reported advancements in cyclability, most of these compounds are hazardous materials and therefore can aggravate the environmental concerns of the LIB value chain. For instance, vinylene carbonate (VC) and divinyl sulfone (DVS) as patented commercial additives [39] are seriously toxic compounds. Therefore, further molecular tunning can be followed to reach a high-performance yet less toxifying chemistry.

In terms of the SEI formation mechanism, a slight modification in molecular structure can cause fundamental changes. When comparing the severe differences between ethylene carbonate (EC) and propylene carbonate (PC) in the interphase formation, it is concluded that the electron-donating effect of the methyl group decreases the capability of the molecule to reduce at an appropriate voltage [6]. On the other hand, replacing the methyl group with the electron-withdrawing fluorine leads to the exact opposite result, where the fluoroethylene carbonate (FEC) reduces at a favorable voltage [12]. Hence, adjusting the electronic arrangement within the molecular structure can be an effective approach to increase the efficiency of additives. Additionally, since the elemental content of the SEI-forming agent determines the eventual interphase composition, controlling the substituents can affect the stability of the reduction products. From another perspective, the SEI-forming reduction–polymerization reactions occur through the generation of radical ions [15,40]. Therefore, the structural properties in terms of radical ion stability are another aspect to consider in molecular design.

Considering the flexible functionalization of the carbonyl group, which gives it interesting chemistry in molecular design, this work is devoted to understanding the performance of its variants in the SEI formation process. In addition, given the environmental footprints of the SEI improving agents, we have targeted studying the performance of less toxic chemistries. The selected structures cover the three different carbonyl derivatives, including carboxylic acid, ester, and acyl halide, so the effects of these functional groups can be compared as a novel approach. In addition, changes caused by the vicinity of the phenyl group to the polymerizable C=C bond are tracked to understand its impact on the

SEI formation process. The performance of the molecules is studied both by computational modeling and electrochemical analysis. It is hoped that our approach contributes to the further development of SEI additives by providing general insight into the impact of the studied substituents.

2. Experiment

2.1. Computational Modeling

Density Functional Theory (DFT) simulations in the Gaussian 16 simulation program package [41] were performed using the B3LYP functional and 6311 g(d, p) basis sets [42] to demonstrate the interaction between Li-ion and different additive molecules. The binding energy was calculated as the energy difference between the optimized lithium–additive complex and single components (i.e., $\Delta E_{bind} = E\left([Li(additive)]^{+}\right) - E(Li^{+}) - E(additive)$). The same functional and basis sets were employed to calculate the energy level of the molecular orbitals.

2.2. Chemicals

Figure 1 displays the molecular structures of the 6 investigated compounds through the SEI formation and evolution process. Cinnamic acid (CIAC), crotonic acid (CRAC), and crotonoyl chloride (CRCL) were purchased from Alfa Aesar. Cinnamoyl chloride (CICL), methyl cinnamate (MECI), and methyl crotonate (MECR) were supplied from Acros Organics. All the solids were vacuum dried in a desiccator for 72 h as opened, and the liquids were directly dried using the activated 4A molecular sieve for 72 h. The base electrolyte was supplied in battery grade from Solvionic, containing a 1M solution of $LiPF_6$ in ethylene carbonate (EC)/dimethyl carbonate (DMC) (1/1, v/v). Each of the 6 modified electrolytes contained 1w% of an SEI-forming compound added to the base electrolyte. All 6 compounds were completely dissolved in the base electrolyte after being stirred for 10 min.

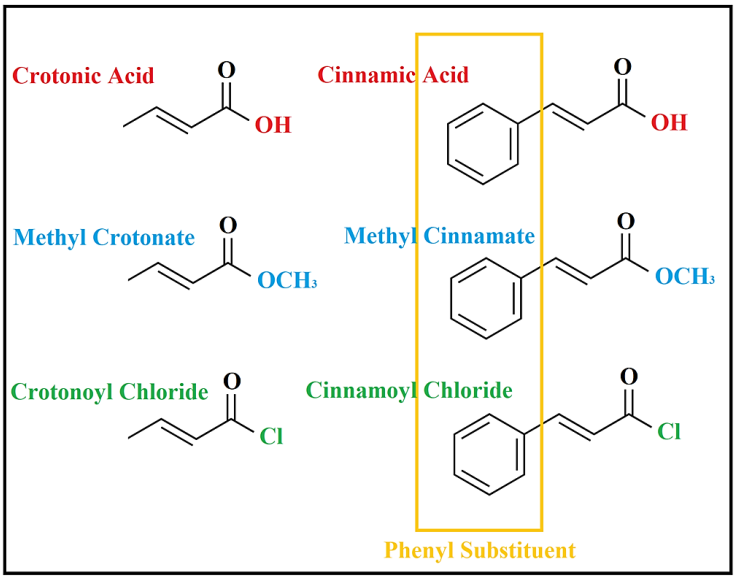

Figure 1. Molecular structures of the studied compounds in the SEI formation process.

2.3. Cell Assembly

To minimize the probable inconsistencies caused by the state of the graphite, a commercial single-side cupper foil-coated CMS graphite electrode (MTI) was applied as the anode for all of the cell configurations. The cathode used in full-cell configuration was prepared by a doctor blade coating of the NMC (532, MTI)/PVDF (Sigma Aldrich)/carbon black (Super P, Alfa Aesar) (90/5/5) slurry on the aluminum foil. The average active material loading was 8.0 and 11.6 mg cm^{-2} for the graphite and the NMC electrodes, respectively.

The electrode preparation was executed inside the dry room (dew point: −45 °C). All the electrodes were vacuum dried before cell assembly and directly transferred to the argon-filled glovebox (H_2O and O_2 concentrations below 1 ppm) where the cell fabrication steps were performed.

2.4. Electrochemical Measurement

Linear sweep voltammetry (LSV) was applied to estimate the oxidation potential of the electrolytes with a three-electrode configuration, using platinum as the working electrode. Lithium and stainless steel were the reference and counter electrode, respectively. Cyclic voltammetry (CV) was carried out in order to verify the reversible intercalation chemistry of the electrolytes and to assess their reduction potentials using a three-electrode configuration, with graphite as the working electrode. Lithium was used as the reference and counter electrode. The voltammetry experiments were implemented with a biologic potentiostaat (VSP) with a scan rate of 0.1 mVs^{-1}. Cyclability of the fabricated coin cells (MTI, 2032) was evaluated in constant-current mode with a biologic battery cycler (BCS). A CTS climate chamber (T-40/50) was used to perform the thermal stability studies.

2.5. Microscopic Imaging

A scanning electron microscope (SEM) was applied (JEOL, JSM-IT300) to observe the interfacial morphology of the graphite electrodes. The graphite/Li half-cells were disassembled in the glovebox, and the collected graphite electrodes were rinsed with DMC three times and then dried for 12 h under a vacuum before SEM analysis.

3. Results and Discussion

3.1. Effects of Substituents on the Oxidation Process

Progress of side reactions by the SEI-forming agents at the positive electrode is understood as an issue which may lead to capacity fade [26,43]. Stability of the electrolyte additives at the cathode could decrease the probability of oxidative decomposition and therefore should be considered an important characteristic for the SEI-forming compounds. When comparing the Highest Occupied Molecular Orbitals (HOMOs), it could be expected that the structures with lower HOMO energy levels have a lower tendency to lose electrons, resulting in more stability against oxidation [44–46].

The calculated HOMO energy level of the selected compounds is summarized by Figure 2a, and the values are compared to those of EC and DMC as the solvent molecules. As is presented by Figure 2a, the expected oxidation stability of the studied molecules followed the order of MECI < CIAC < CICL < MECR < CRAC < CRCL.

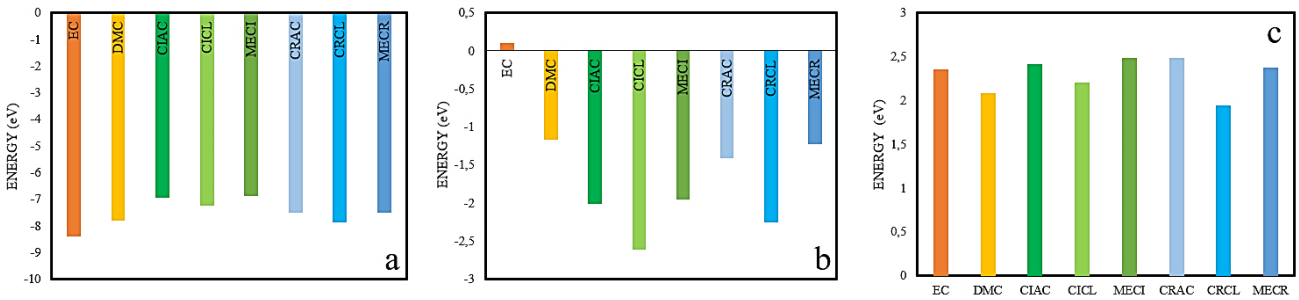

Figure 2. Comparing the energy level of the HOMO (**a**) and LUMO (**b**) molecular orbitals and the lithium-binding energy (**c**) of the studied structures with the base electrolyte solvents.

On the other hand, the anodic stability of the SEI-forming agents was evaluated using linear sweep voltammetry (LSV), as shown by Figure 3. The LSV result of the base electrolyte is also presented for comparison. As can be seen by the LSV plot and the HOMO energy values, structures containing a phenyl group had lower oxidation stability compared with those without this substituent. Therefore, both the LSV experiment and

DFT modeling suggest that proximity of the phenyl group to the unsaturated C=C bond decreased the oxidation stability of the structure. This could be explained by the radical ion stabilizing effect of the aromatic cycle through charge delocalization. From another perspective, the observed differences in oxidation stability of acyl halide, carboxylic acid, and ester could be rationalized by the differences in the electron-withdrawing effect of these functional groups. Regarding the low oxidation potential of MECI, it would not be stable against oxidative decomposition. The other compounds, however, showed acceptable stability in the potential range of the 4.2-V LIBs.

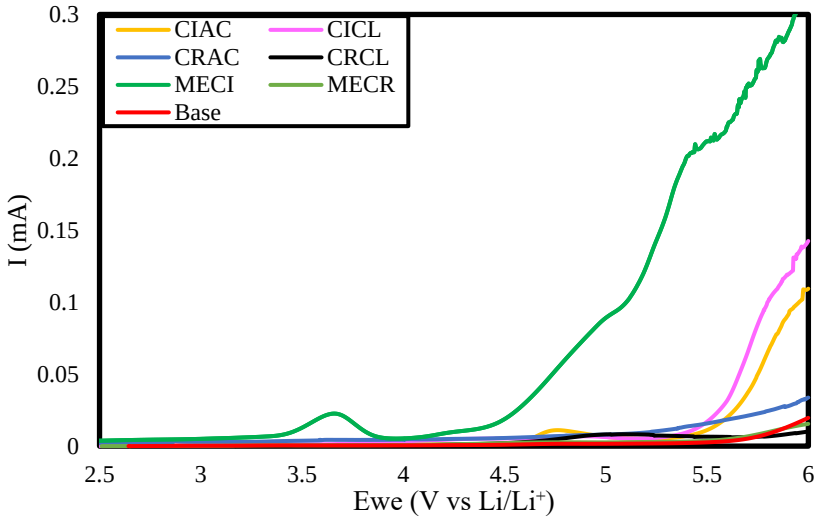

Figure 3. Comparing the oxidation stabilities of the selected SEI-forming compounds with the base electrolyte through the LSV experiment.

3.2. Effects of Substituents on the Reduction Process

Figure 4 compares the cyclic voltammetry results of the SEI-forming agents with the base electrolyte. As can be seen in the plots, all the studied compounds provided a reversible Li^+ ion intercalation chemistry at the graphite anode. The lithium-binding energy of the electrolyte components is an important factor to determine the reversibility of the (de)intercalation process, where high interactions of a molecule with Li^+ ions can result in its co-intercalation [47,48], leading to electrode instability and capacity loss. As presented in Figure 2c, the DFT calculations suggested lower lithium binding energies for CRCL and CICL among all the considered structures.

Comparing the reduction potential of the applied SEI-forming agents with the base electrolyte, it could be seen that all of these compounds initiated the decomposition reactions prior to the solvent molecules (i.e., they would participate in the SEI formation process). The tendency of molecules to carry out the reduction reaction could be predicted by comparing the energy level of the Lowest Unoccupied Molecular Orbitals (LUMOs), where lower values are interpreted as easier reduction pathways [19,45,46,49]. As is shown in Figure 2b, DFT modeling calculated the LUMO energy levels, in order, as CICL < CRCL < CIAC < MECI < CRAC < MECR, which is in agreement with the CV results. This order, from one side, could be related to the electron-withdrawing effect of the functional groups, where the acyl chlorides showed a higher reduction tendency compared with the carboxylic acids and esters. From another point of view, conjugation of the unsaturated C=C bond with the phenyl group, which delocalizes the charge within the structure and stabilizes the radical ion intermediates, could explain the observation for SEI formation. The CV plots also showed that the SEI formation process mainly proceeded through the first cycle.

Regarding the appearing phenomena through the CV analysis, a voltage shift could be detected in the oxidation potential as the cells were cycled. We think this effect, which has been more traceable in the case of MECI, CICL, and CRAC is originating from the changes in electrode polarization through the deintercalation process as the cell cycled, and the

lowered anodic polarization could be attributed to the gradual surface stabilization as the SEI was developed.

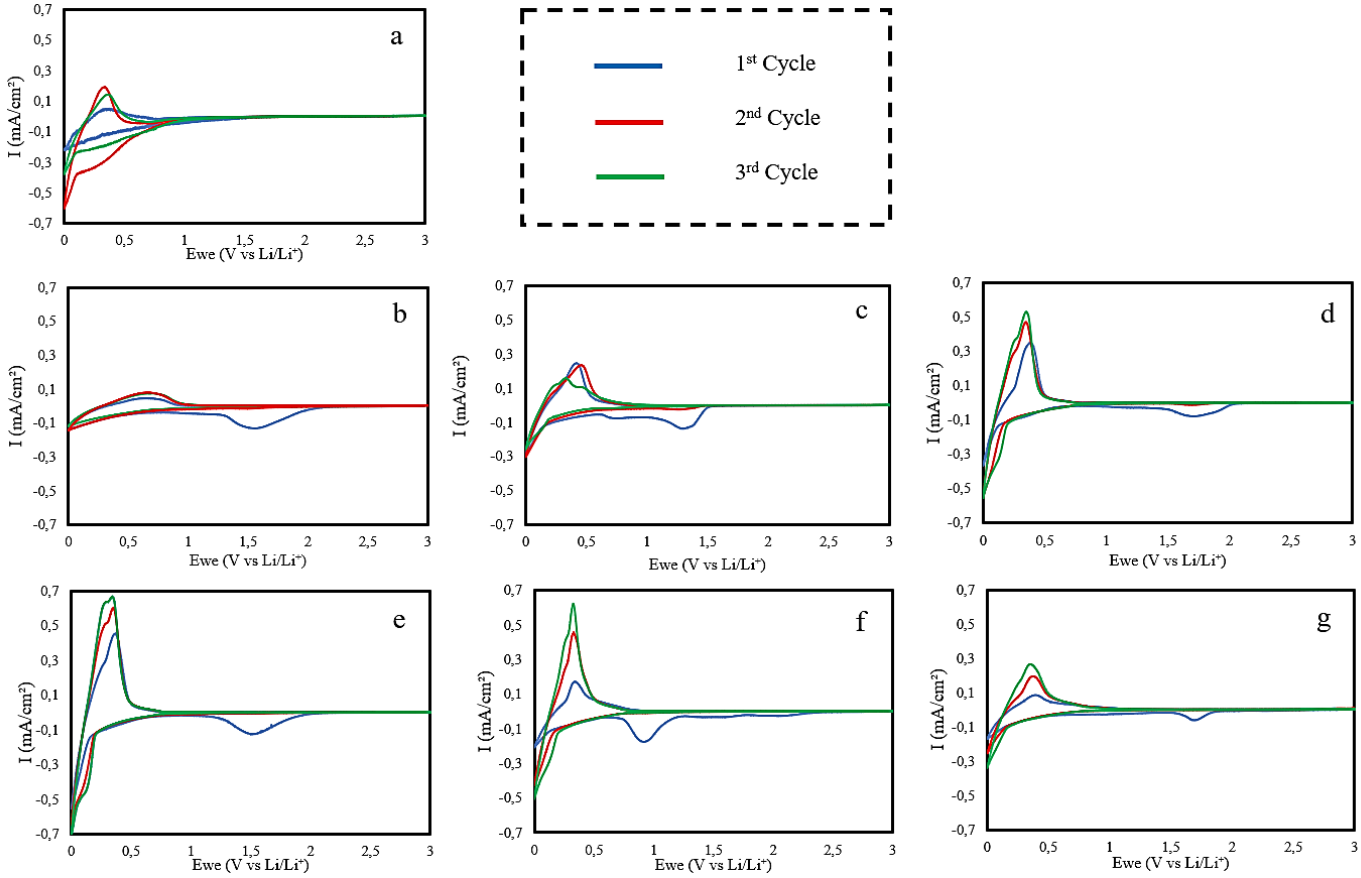

Figure 4. Comparing the CV plots of the base electrolyte without SEI-forming compounds (**a**) with those containing 1w% of CIAC (**b**), MECI (**c**), CICL (**d**), CRAC (**e**), MECR (**f**), and CRCL (**g**).

3.3. Cycle Performance of the Graphite/Lithium Half-Cells

Cyclability of the half-cells was investigated among the base and the modified electrolytes to understand the effects of the different substituents on the graphite SEI formation and its intercalation chemistry. Figure 5 presents the cycle performances of the graphite/lithium coin cells at room temperature. The modified electrolytes contained 1w% of different SEI-forming compounds added to the base solution. The total capacity loss for each electrolyte during the SEI formation stage is shown in Figure 5a with respect to the initial nominal capacity of the cells. The assembled coin cells were cycled six times in this level with the low current rate of 0.05C. Changes that happened in the capacity retention and the coulombic efficiency after the half-cell interphase formation are plotted by Figure 5b,c, respectively, where the SEI layer gradually evolved. The coin cells were cycled for 10 cycles with a C-rate of 0.1C at this stage, followed by another 10 cycles with a higher C-rate of 0.2C.

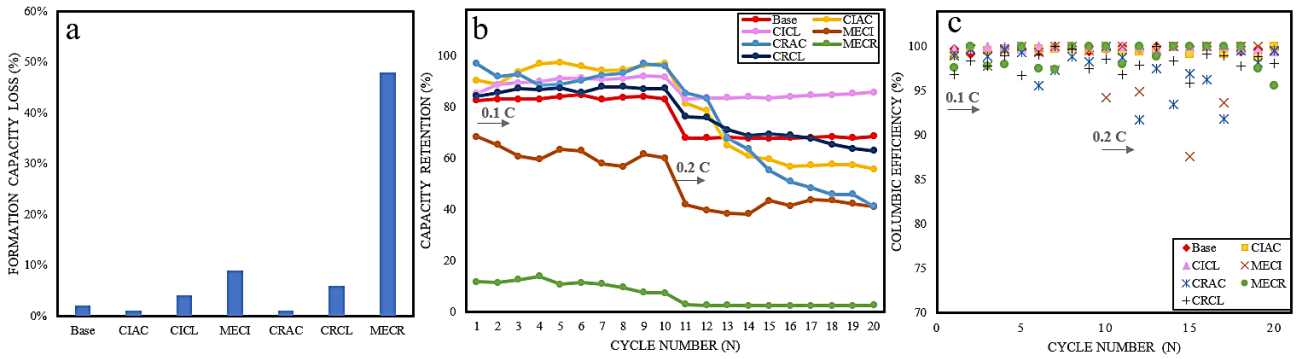

Figure 5. Comparing the cycle performance of the modified electrolytes with the base electrolyte in a half-cell configuration. The initial capacity loss during the SEI formation step (**a**), the capacity retention of the cells after the interphase formation (**b**), and the relevant columbic efficiency (**c**) are shown.

In general, the addition of the ester compounds caused higher levels of initial capacity loss. However, there was a significant gap between MECR and MECI, where MECR suffered a 48% capacity drop, leading to unacceptable graphite interphase formation. MECI showed 9% initial capacity loss in this term. When comparing the performance of carboxylic acids with acyl halides, despite the slightly higher capacity loss caused by reduction of the acyl chlorides, all four compounds resulted in capacity drops lower than 6%. The initial capacity loss caused by the base electrolyte was 2%. As is depicted in Figure 5, in all samples, increasing the C-rate during the evolution stage decreased the capacity of the coin cells. In comparison with the base solution, the electrolyte modified with CICL presented better capacity retention. The 0.1C cycle performance of the studied half-cells followed the order of MECR < MECI < base electrolyte < CRCL < CICL < CRAC < CIAC. However, when raising the C-rate to 0.2C, CICL was the only SEI-forming agent which improved and maintained the capacity retention.

When comparing the cell properties after the cycles, we noticed a decrease in the OCV value for the ones containing carboxylic acid (1.1–1.4 V). Regarding the dropped capacity in those cases, we think that the observed phenomenon could be attributed to the partial lithium plating at the graphite electrode [46]. Considering the correlation between lithium plating and the kinetics of the intercalation process, the state of the SEI layer affects this process, where formation of inefficient interphase assists the lithium deposition reaction [50,51]. It could be concluded that by increasing the current rate, gradual lithium deposition at the graphite electrode negatively impacted the cell performance.

To investigate the state of the formed SEI layers in terms of morphology, SEM imaging was implemented after the formation cycles. The pictures captured from the surfaces of the graphite electrodes are presented in Figure 6. As can be seen in the pictures, the progress of the SEI formation cycles resulted in the formation of a thin film covering the graphite particles. As a general observation, the SEI layers formed by CICL and CRCL seemed smoother, whereas those formed by the other electrolytes featured rougher surfaces. Additionally, precipitation of a powder-like white species was seen with the addition of CICL and CRCL. This observation, which was more distinctive in the case of CRCL, might represent LiCl as an inorganic decomposition product, but a certain answer requires further compositional analysis, which is out of the scope of this work.

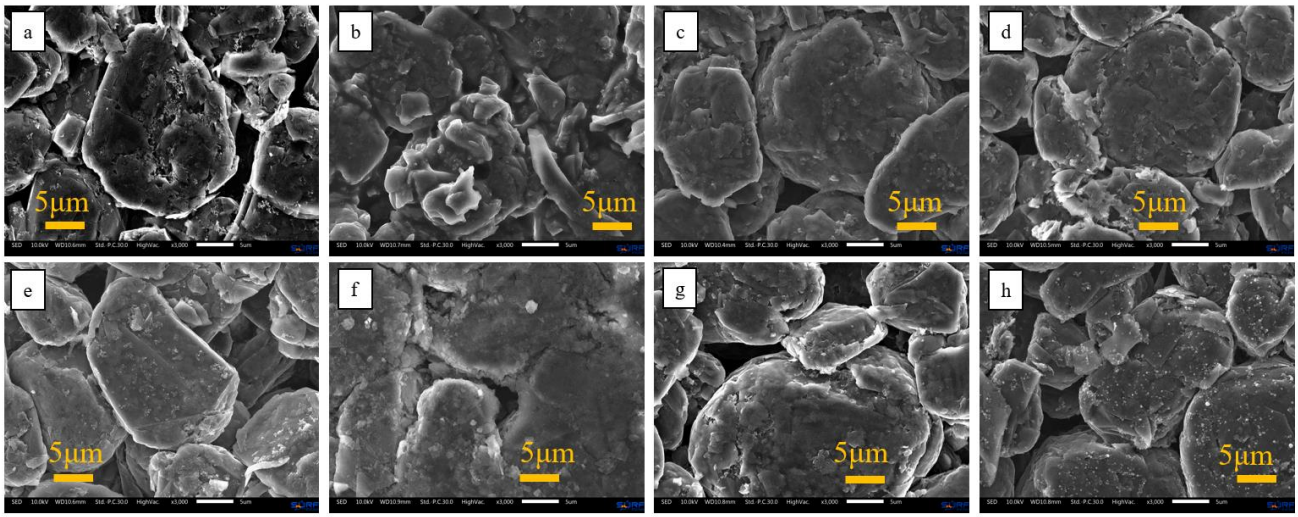

Figure 6. SEM pictures of the de-lithiated graphite anodes, showing the fresh electrode (**a**) and the electrodes after the formation cycles in the base electrolyte (**b**) as well as the electrolytes containing CIAC (**c**), MECI (**d**), CICL (**e**), CRAC (**f**), MECR (**g**), and CRCL (**h**).

3.4. Cycle Performance of the NMC/Graphite Full Cells

The effects of the different substituents on the cyclability of the full-cell configuration LIBs were investigated after the formation cycles. Figure 7 presents the cycle performances of NMC/graphite coin cells at room temperature with the electrolytes containing 1w% of different SEI-forming compounds. The results of the base electrolyte are also presented for comparison. Figure 7a shows the total capacity loss for each electrolyte during the SEI formation stage with respect to the initial nominal capacity of the cell. The fabricated coin cells were cycled for six cycles in this step with a low current rate of 0.05C. Changes that occurred in the capacity retention and the coulombic efficiency of the full cells after the SEI formation are plotted in Figure 7b,c, respectively. This stage was considered the SEI evolution process, where the cells were cycled for 20 cycles with a C-rate of 0.1C, followed by 20 cycles with a higher C-rate of 0.2C. As is depicted in Figure 7, in all cases, increasing the C-rate during the evolution stage decreased the capacity of the cell. The results show that the initial capacity loss during the SEI formation cycles was drastically increased in comparison with those of the half-cell configurations. This clearly shows that in shifting from the lithium foil to the NMC electrodes, the capacity loss was intensified due to the limitations of the lithium inventory. The addition of CICL to the electrolyte, however, considerably decreased this issue, as it featured the least drop in capacity with a value of 10%. MECR on the other hand caused 63% of the initial capacity loss during the SEI formation step.

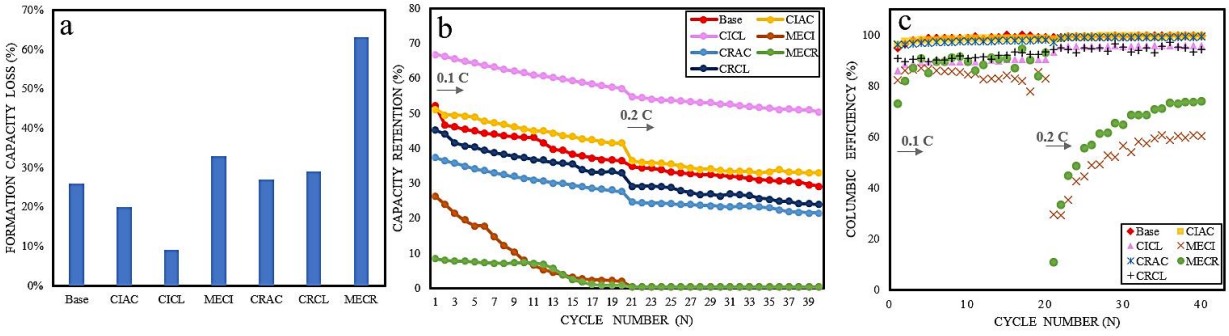

Figure 7. Comparing the cycle performance of the modified electrolytes with the base electrolyte in a full-cell configuration. The initial capacity loss during the SEI formation step (**a**), the capacity retention of the cells after the interphase formation (**b**), and the relevant columbic efficiency (**c**) are shown.

Comparing the two sides of this spectrum shows that in the case of CICL, a stable SEI layer was formed in a controlled process, but the presence of MECR in the system resulted in a continuoued electrolyte decomposition process. This trend continued in the evolution step, where CICL significantly improved the capacity retention of the base electrolyte (both at 0.1C and 0.2C), but MECR caused a quick drop in the applicable capacity of the coin cell. The performance of the studied electrolytes followed an order of MECR < MECI < CRAC < CRCL < base electrolyte < CIAC < CICL. The addition of the ester compounds (i.e., MECI and MECR) immediately decreased the cell capacity. By tracking the changes that occurred in the columbic efficiency of the coin cells, it could be seen that the ester compounds pursued a continued decomposition even at later evolution steps. This feature, which intensified at higher current rates, could be explained by the formation of an unstable interphase, leading to a drastic ICL and eventually a quick end of life.

The cyclic performance of the NMC/graphite coin cells was investigated at 45 °C after the formation cycles to track the effect of the elevated temperature on the SEI stability. All the cells were kept inside the climate chamber at the testing temperature for 1 h before starting the measurement. The cells were cycled for 10 cycles with a C-rate of 0.1C, followed by 10 cycles with an increased current rate of 0.2C. The capacity retention was reported after the formation cycles with respect to the initial nominal capacities of the cells. As depicted in Figure 8, among the compounds which had ameliorated the cyclic performance of the electrolyte at a higher temperature, CICL brought more improvement to the capacity retention. This could be interpreted as the formation of an SEI featuring improved thermal stability in the case of CICL reduction.

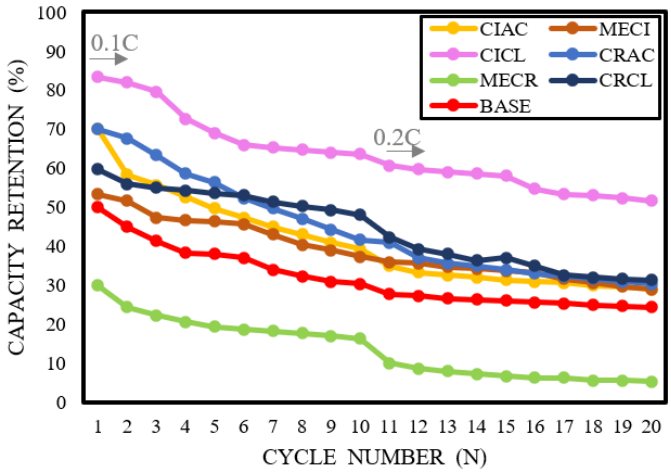

Figure 8. Comparing the cyclic performance of the base and the modified electrolytes at 45 °C.

4. Summary and Outlook

4.1. Conclusions

Changes in the electronic properties of the molecular structure were tracked and compared for three different functional groups, including carboxylic acid, ester, and acyl halide as SEI-forming compounds. The obtained results from the DFT modeling and the electrochemical analysis confirmed that substitution of a group with a higher tendency for an electron-withdrawing effect facilitated the reduction pathway of the molecule as a necessary feature in the SEI-forming process. The results of the lithium-binding energy calculation for different carbonyl derivatives showed that the acyl halide group had a lower interaction with the Li^+ ions, which decreased the probability of co-intercalation and could prevent gradual electrode exfoliation. It was also found that the proximity of the phenyl substituent could lead to more efficient SEI formation, expectedly through stabilization of the radical ion intermediates. This feature, however, could facilitate the oxidation pathways for the structure, where the vicinity of a strong electron-withdrawing group could balance out this effect on some levels.

Based on the cyclability assessments, cinnamoyl chloride (CICL) could be considered a potential SEI-forming agent, which ameliorated the SEI properties both at room temperature and at 45 °C yet featured less toxic chemistry in comparison with common SEI additives.

4.2. Future Work

When comparing the cyclic behavior of the studied electrolytes, the results suggest that cinnamoyl chloride could form a more stable SEI layer, leading to better capacity retention. Given the significance of sustainability in the battery value chain, reduced environmental drawbacks of such compounds could be considered an important approach to follow in order to improve the practical applicability of LIB electrolytes.

Coupling the computational and electrochemical investigations with further compositional studies could be followed to certify the predicted origin of the improved interphase stability. For being able to detect the elemental composition of the interphase and track the type of bonds between them, X-ray photoelectron spectroscopy could be proposed as a research approach to perform further investigation on the chemical nature of the SEI layer. Additionally, the obtained information about the effects of the studied substituents on the SEI formation process could be engaged in molecular tunning to develop other SEI-improving additives.

Author Contributions: Conceptualization, methodology, investigation, validation, formal analysis and writing—original draft preparation by S.H.B.; Computational modeling by S.H.B. and M.H.M.; Writing—review and editing by M.J., H.O., H.B., X.Z., M.H.M., A.H., J.V.M. and M.B.; Supervision by M.J., H.O., A.H., J.V.M. and M.B. All authors have read and agreed to the published version of the manuscript.

Funding: This research received no external funding.

Acknowledgments: M.H.M. acknowledges funding from the Fonds Wetenschappelijk Onderzoek in Flanders (FWO, project 1264221N).

Conflicts of Interest: The authors declare no conflict of interest.

References

1. Funabiki, A.; Inaba, M.; Abe, T.; Ogumi, Z. Stage Transformation of Lithium-Graphite Intercalation Compounds Caused by Electrochemical Lithium Intercalation. *J. Electrochem. Soc.* **1999**, *146*, 2443–2448. [CrossRef]
2. Peled, E.; Golodnitsky, D.; Ardel, G. Advanced Model for Solid Electrolyte Interphase Electrodes in Liquid and Polymer Electrolytes. *J. Electrochem. Soc.* **1997**, *144*, L208–L210. [CrossRef]
3. Peled, E.; Menkin, S. Review—SEI: Past, Present and Future. *J. Electrochem. Soc.* **2017**, *164*, A1703–A1719. [CrossRef]
4. Verma, P.; Maire, P.; Novák, P. A review of the features and analyses of the solid electrolyte interphase in Li-ion batteries. *Electrochim. Acta* **2010**, *55*, 6332–6341. [CrossRef]
5. Heiskanen, S.; Kim, J.; Lucht, B.L. Generation and Evolution of the Solid Electrolyte Interphase of Lithium-Ion Batteries. *Joule* **2019**, *3*, 2322–2333. [CrossRef]
6. Xu, K. Electrolytes and Interphases in Li-Ion Batteries and Beyond. *Chem. Rev.* **2014**, *114*, 11503–11618. [CrossRef]
7. Zuo, W.; Cui, Y.; Zhuang, Q.; Shi, Y.; Ying, P.; Cui, Y. Effect of N-N Dimethyltrifluoroacetamide Additive on Low Temperature Performance of Graphite Anode. *Int. J. Electrochem. Sci.* **2020**, *15*, 382–393. [CrossRef]
8. Zhao, L.; Jing, D.; Shi, Y.; Zhuang, Q.; Cui, Y.; Ju, Z.; Cui, Y. TriMethylene sulfite as a novel additive for SEI film formation in lithium-ion batteries. *Ionics* **2020**, *26*, 4813–4824. [CrossRef]
9. Edstroem, K.; Herstedt, M.; Abraham, D.P. A new look at the solid electrolyte interphase on graphite anodes in Li-ion batteries. *J. Power Sources* **2006**, *153*, 380–384. [CrossRef]
10. Lu, P.; Li, C.; Schneider, E.W.; Harris, S.J. Chemistry, Impedance, and Morphology Evolution in Solid Electrolyte Interphase Films during Formation in Lithium Ion Batteries. *J. Phys. Chem. C* **2014**, *118*, 896–903. [CrossRef]
11. Takenaka, N.; Suzuki, Y.; Sakai, H.; Nagaoka, M. On Electrolyte-Dependent Formation of Solid Electrolyte Interphase Film in Lithium-Ion Batteries: Strong Sensitivity to Small Structural Difference of Electrolyte Molecules. *J. Phys. Chem. C* **2014**, *118*, 10874–10882. [CrossRef]
12. Michan, A.L.; Parimalam, B.S.; Leskes, M.; Kerber, R.N.; Yoon, T.; Grey, C.; Lucht, B.L. Fluoroethylene Carbonate and Vinylene Carbonate Reduction: Understanding Lithium-Ion Battery Electrolyte Additives and Solid Electrolyte Interphase Formation. *Chem. Mater.* **2016**, *28*, 8149–8159. [CrossRef]

13. Schwenke, K.U.; Soc, J.E.; Schwenke, K.U.; Solchenbach, S.; Gasteiger, H.A.; Demeaux, J.; Lucht, B.L. The Impact of CO 2 Evolved from VC and FEC during Formation of Graphite Anodes in Lithium-Ion Batteries. The Impact of CO 2 Evolved from VC and FEC during Formation of Graphite Anodes in Lithium-Ion Batteries. *J. Electrochem. Soc.* **2019**, *166*, A2035. [CrossRef]
14. Shkrob, I.A.; Zhu, Y.; Marin, T.W.; Abraham, D. Reduction of Carbonate Electrolytes and the Formation of Solid-Electrolyte Interface (SEI) in Lithium-Ion Batteries. 2. Radiolytically Induced Polymerization of Ethylene Carbonate. *J. Phys. Chem. C* **2013**, *117*, 19270–19279. [CrossRef]
15. Korepp, C.; Kern, W.; Lanzer, E.; Raimann, P.; Besenhard, J.; Yang, M.; Möller, K.-C.; Shieh, D.-T.; Winter, M. Isocyanate compounds as electrolyte additives for lithium-ion batteries. *J. Power Sources* **2007**, *174*, 387–393. [CrossRef]
16. Zhang, S.S. A review on electrolyte additives for lithium-ion batteries. *J. Power Sources* **2006**, *162*, 1379–1394. [CrossRef]
17. Wang, R.; Li, X.; Wang, Z.; Zhang, H. Electrochemical analysis graphite/electrolyte interface in lithium-ion batteries: P-Toluenesulfonyl isocyanate as electrolyte additive. *Nano Energy* **2017**, *34*, 131–140. [CrossRef]
18. Zuo, X.; Deng, X.; Ma, X.; Wu, J.; Liang, H.; Nan, J. 3-(Phenylsulfonyl)propionitrile as a higher voltage bifunctional electrolyte additive to improve the performance of lithium-ion batteries. *J. Mater. Chem. A* **2018**, *6*, 14725–14733. [CrossRef]
19. Shi, J.; Ehteshami, N.; Ma, J.; Zhang, H.; Liu, H.; Zhang, X.; Li, J.; Paillard, E. Improving the graphite/electrolyte interface in lithium-ion battery for fast charging and low temperature operation: Fluorosulfonyl isocyanate as electrolyte additive. *J. Power Sources* **2019**, *429*, 67–74. [CrossRef]
20. Li, Z.; Lin, X.; Zhou, H.; Xing, L.; Lan, G.; Zhang, W.; Chen, J.; Liu, M.; Huang, Q.; Li, W. Stabilizing the interphasial layer of Ni-rich cathode and graphite anode for lithium ion battery with multifunctional additive. *J. Power Sources* **2020**, *467*, 228343. [CrossRef]
21. Li, X.; Guo, L.; Li, J.; Wang, E.; Liu, T.; Wang, G.; Sun, K.; Liu, C.; Peng, Z. Reversible Cycling of Graphite Electrodes in Propylene Carbonate Electrolytes Enabled by Ethyl Isothiocyanate. *ACS Appl. Mater. Interfaces* **2021**, *13*, 26023–26033. [CrossRef]
22. Nie, M.; Demeaux, J.; Young, B.; Heskett, D.R.; Chen, Y.; Bose, A.; Woicik, J.C.; Lucht, B.L. Effect of Vinylene Carbonate and Fluoroethylene Carbonate on SEI Formation on Graphitic Anodes in Li-Ion Batteries. *J. Electrochem. Soc.* **2015**, *162*, A7008–A7014. [CrossRef]
23. Winkler, V.; Hanemann, T.; Bruns, M. Comparative surface analysis study of the solid electrolyte interphase formation on graphite anodes in lithium-ion batteries depending on the electrolyte composition. *Surf. Interface Anal.* **2017**, *49*, 361–369. [CrossRef]
24. Zhao, X.; Zhuang, Q.; Xu, S.; Xu, Y.; Shi, Y.; Zhang, X. A New Insight into the Content Effect of Fluoroethylene Carbonate as a Film Forming Additive for Lithium-Ion Batteries. *Int. J. Electrochem. Sci.* **2015**, *10*, 2515–2534.
25. Chang, C.-C.; Hsu, S.-H.; Jung, Y.-F.; Yang, C.-H. Vinylene carbonate and vinylene trithiocarbonate as electrolyte additives for lithium ion battery. *J. Power Sources* **2011**, *196*, 9605–9611. [CrossRef]
26. Jung, H.M.; Park, S.-H.; Jeon, J.; Choi, Y.; Yoon, S.; Cho, J.-J.; Oh, S.; Kang, S.; Han, Y.-K.; Lee, H. Fluoropropane sultone as an SEI-forming additive that outperforms vinylene carbonate. *J. Mater. Chem. A* **2013**, *1*, 11975–11981. [CrossRef]
27. Wang, L.; Liu, S.; Zhao, K.; Li, J.; Yang, Y.; Jia, G. Improving the rate performance and stability of LiNi0.6Co0.2Mn0.2O2 in high voltage lithium-ion battery by using fluoroethylene carbonate as electrolyte additive. *Ionics* **2018**, *24*, 3337–3346. [CrossRef]
28. Shin, H.; Park, J.; Sastry, A.M.; Lu, W. Effects of Fluoroethylene Carbonate (FEC) on Anode and Cathode Interfaces at Elevated Temperatures. *J. Electrochem. Soc.* **2015**, *162*, A1683–A1692. [CrossRef]
29. Ufheil, J.; Baertsch, M.C.; Würsig, A.; Novák, P. Maleic anhydride as an additive to γ-butyrolactone solutions for Li-ion batteries. *Electrochim. Acta* **2005**, *50*, 1733–1738. [CrossRef]
30. Santner, H.; Möller, K.-C.; Ivančo, J.; Ramsey, M.; Netzer, F.; Yamaguchi, S.; Besenhard, J.; Winter, M. Acrylic acid nitrile, a film-forming electrolyte component for lithium-ion batteries, which belongs to the family of additives containing vinyl groups. *J. Power Sources* **2003**, *119–121*, 368–372. [CrossRef]
31. Korepp, C.; Santner, H.; Fujii, T.; Ue, M.; Besenhard, J.; Möller, K.-C.; Winter, M. 2-Cyanofuran—A novel vinylene electrolyte additive for PC-based electrolytes in lithium-ion batteries. *J. Power Sources* **2006**, *158*, 578–582. [CrossRef]
32. Yong, T.; Wang, J.; Mai, Y.; Tang, D.; Zhang, L. Allyl cyanide as a new functional additive in propylene carbonate-based electrolyte for lithium-ion batteries. *Ionics* **2013**, *19*, 1099–1103. [CrossRef]
33. Liu, W.; Shi, Y.; Zhuang, Q.; Cuiab, Y.; Ju, Z.; Cui, Y. Ethylene Glycol Bis(Propionitrile) Ether as an Additive for SEI Film Formation in Lithium-Ion Batteries. *Int. J. Electrochem. Sci.* **2020**, *15*, 4722–4738. [CrossRef]
34. Korepp, C.; Kern, W.; Lanzer, E.; Raimann, P.; Besenhard, J.; Yang, M.; Möller, K.-C.; Shieh, D.-T.; Winter, M. Ethyl isocyanate—An electrolyte additive from the large family of isocyanates for PC-based electrolytes in lithium-ion batteries. *J. Power Sources* **2007**, *174*, 628–631. [CrossRef]
35. Lee, H.; Choi, S.; Choi, S.; Kim, H.-J.; Choi, Y.; Yoon, S.; Cho, J.-J. SEI layer-forming additives for LiNi0.5Mn1.5O4/graphite 5V Li-ion batteries. *Electrochem. Commun.* **2007**, *9*, 801–806. [CrossRef]
36. Xu, M.; Zuo, X.; Li, W.; Zhou, H.; Liu, J.; Yuan, Z. Effect of Butyl Sultone on the Li-ion Battery Performance and Interface of Graphite Electrode. *Acta Phys.-Chim. Sin.* **2006**, *22*, 335–340. [CrossRef]
37. Mai, S.; Xu, M.; Wang, Y.; Liao, X.; Lin, H.; Li, W. Methylene methanedisulfonate (MMDS) as a novel SEI forming additive on anode for lithium ion batteries. *Int. J. Electrochem. Sci.* **2014**, *9*, 6294–6304.
38. Högström, K.C.; Hahlin, M.; Malmgren, S.; Gorgoi, M.; Rensmo, H.; Edström, K. Aging of Electrode/Electrolyte Interfaces in LiFePO4/Graphite Cells Cycled with and without PMS Additive. *J. Phys. Chem. C* **2014**, *118*, 12649–12660. [CrossRef]

39. Ershadi, M.; Javanbakht, M.; Beheshti, S.H.R.; Mosallanejad, B.; Kiaei, Z. A patent landscape on liquid electrolytes for lithium-ion batteries. *Anal. Bioanal. Electrochem.* **2018**, *10*, 1629–1653.
40. Strehle, B.; Solchenbach, S.; Metzger, M.; Schwenke, K.U.; Gasteiger, H.A. The Effect of CO_2 on Alkyl Carbonate Trans-Esterification during Formation of Graphite Electrodes in Li-Ion Batteries. *J. Electrochem. Soc.* **2017**, *164*, A2513–A2526. [CrossRef]
41. Frisch, M.; Trucks, G.; Schlegel, H.; Scuseria, G.; Robb, M.; Cheeseman, J.; Scalmani, G.; Barone, V.; Petersson, G.; Nakatsuji, H.; et al. *Gaussian 16, Revision A.03*; Gaussian, Inc.: Wallingford, CT, USA, 2016.
42. Becke, A.D. Density-functional thermochemistry. The role of exact exchange. *J. Chem. Phys.* **1993**, *98*, 5648–5652. [CrossRef]
43. Yoon, S.; Kim, H.; Cho, J.-J.; Han, Y.-K.; Lee, H. Lactam derivatives as solid electrolyte interphase forming additives for a graphite anode of lithium-ion batteries. *J. Power Sources* **2013**, *244*, 711–715. [CrossRef]
44. Zhang, Z.; Hu, L.; Wu, H.; Weng, W.; Koh, M.; Redfern, P.C.; Curtiss, L.A.; Amine, K. Fluorinated electrolytes for 5 V lithium-ion battery chemistry. *Energy Environ. Sci.* **2013**, *6*, 1806–1810. [CrossRef]
45. Goodenough, J.B.; Kim, Y. Challenges for Rechargeable Li Batteries. *Chem. Mater.* **2010**, *22*, 587–603. [CrossRef]
46. Khasanov, M.; Pazhetnov, E.; Shin, W.C. Dicarboxylate-Substituted Ethylene Carbonate as an SEI-Forming Additive for Lithium-Ion Batteries. *J. Electrochem. Soc.* **2015**, *162*, A1892–A1898. [CrossRef]
47. Park, M.H.; Lee, Y.S.; Lee, H.; Han, Y.-K. Low Li+ binding affinity: An important characteristic for additives to form solid electrolyte interphases in Li-ion batteries. *J. Power Sources* **2011**, *196*, 5109–5114. [CrossRef]
48. Wang, A.; Kadam, S.; Li, H.; Shi, S.; Qi, Y. Review on modeling of the anode solid electrolyte interphase (SEI) for lithium-ion batteries. *npj Comput. Mater.* **2018**, *4*, 15. [CrossRef]
49. Zhang, Z.; Smith, K.; Jervis, R.; Shearing, P.R.; Miller, T.S.; Brett, D.J.L. Operando Electrochemical Atomic Force Microscopy of Solid–Electrolyte Interphase Formation on Graphite Anodes: The Evolution of SEI Morphology and Mechanical Properties. *ACS Appl. Mater. Interfaces* **2020**, *12*, 35132–35141. [CrossRef]
50. Bugga, R.V.; Smart, M.C. Lithium Plating Behavior in Lithium-Ion Cells. *ECS Trans.* **2010**, *25*, 241–252. [CrossRef]
51. Smart, M.C.; Ratnakumar, B.V. Effects of Electrolyte Composition on Lithium Plating in Lithium-Ion Cells. *J. Electrochem. Soc.* **2011**, *158*, A379–A389. [CrossRef]